INTERNATIONAL JOURNAL OF
ENERGY AND ENVIRONMENT

Volume 6, Issue 5, 2015 pp.437-460
Journal homepage: www.IJEE.IEEFoundation.org

Classification of textures in satellite image with Gabor filters and a multi layer perceptron with back propagation algorithm obtaining high accuracy

Adriano Beluco[1], Paulo M. Engel[2], Alexandre Beluco[3]

[1] Centro Estadual de Pesquisas em Sensoriamento Remoto e Meteorologia (CEPSRM), Universidade Federal Rio Grande do Sul (UFRGS), Porto Alegre, Brazil.
[2] Curso de Pós graduação em Ciências da Computação, Universidade Federal Rio Grande do Sul (UFRGS), Porto Alegre, Brazil.
[3] Instituto de Pesquisas Hidráulicas (IPH), Universidade Federal Rio Grande do Sul (UFRGS), Porto Alegre, Brazil.

Abstract
The classification of images, in many cases, is applied to identify an alphanumeric string, a facial expression or any other characteristic. In the case of satellite images is necessary to classify all the pixels of the image. This article describes a supervised classification method for remote sensing images that integrates the importance of attributes in selecting features with the efficiency of artificial neural networks in the classification process, resulting in high accuracy for real images. The method consists of a texture segmentation based on Gabor filtering followed by an image classification itself with an application of a multi layer artificial neural network with a back propagation algorithm. The method was first applied to a synthetic image, like training, and then applied to a satellite image. Some results of experiments are presented in detail and discussed. The application of the method to the synthetic image resulted in the identification of 89.05% of the pixels of the image, while applying to the satellite image resulted in the identification of 85.15% of the pixels. The result for the satellite image can be considered a result of high accuracy.

Keywords: Remote sensing; Neural networks; Gabor filter; Texture; Image processing; Image classification.

1. Introduction

The traditional classification procedures based on the spectral image attributes may encounter difficulties with classes with similar characteristics. The image spatial attributes like texture may contribute to increase classification accuracy. A possible definition for texture consists of describing it as a repetition of elementary patterns, but a better statement [1] is: “a region in an image has a constant texture if a set of local statistics or other local properties of the picture are constant, slowly varying or approximately periodic”.
The image classification based on texture shall be performed in two stages. First, a procedure for extraction of texture characteristics. The properties of a texture can be efficiently obtained using a properly set of Gabor filters, with appropriately chosen frequency, size and orientation for the filters.

Second, a procedure for classification of image to rebuild the original image. The neural networks allow detect easily any functional relationship between its input and its output patterns and they spare the need to express that relationship explicitly. No assumptions need to be made about the statistical distributions underlying the input patterns.

Reference [2] proposed an algorithm inspired on the multi channel filtering technique for unsupervised texture segmentation, which uses a bank of Gabor filters to characterize the textural channels. For this purpose it employ a systematic filter selection scheme based on the reconstruction of the input image through the filtered images. A clustering algorithm is used for classification purposes.

Reference [3] presented a two-stage neural network structure, combining the characteristics of a self organizing map with a multi layer perceptron. In a previous stage, they also use a multi channel filtering technique to extract textural characteristics, based on a bank of Gabor filters. The self organizing map neural network is used as a clustering mechanism to map the information about texture bands. The multi layer neural network is used for training and subsequent image classification. This mechanism increases the interclass distance and at the same time decreases the intraclass distance.

These two works consist of unsupervised methods. The determination of parameters from the choice of samples of classes to be identified can raise the classification accuracy. Reference [4] used the multi channel filtering technique, through Gabor filters, together with the maximum Gaussian likelihood to propose a supervised segmentation method, based on textural attributes. Unlike the two approaches above, this approach based the selection of parameters in the choice of samples.

Other articles also dealing with texture segmentation by Gabor filters [5, 6] or classification by neural networks [7, 8], with supervised [7, 8] or unsupervised [9, 10] methods. The approach in Reference [7] was based on the extraction of texture features with a bank of Gabor filters of different frequencies, resolutions and orientations, following by its segmentation with a three dimensional Hopfield network with a maximum a posteriori probability criteria. The segmentation consisted of feature formation, feature partition and feature competition processes. In the formation and partition processes, respectively, the features was modeled as a Gaussian distribution and represented by means of a noncausal Markov random field. The competition process forces each pixel to belong to just a feature.

Reference [8] also proposed a very similar method, using stochastic relaxation neural network. Reference [9] describes an unsupervised method for classification of textures using image specific constraints. Reference [10] also deals with the classification of textures by means of neural networks.

There are interesting applications of Gabor filters in other areas, dealing with facial imagery recognition and classification [11, 12], also dealing with Gabor filters followed by neural networks [13], dealing with license plate identification [14], with apple quality inspection [15], with getting information for soil loss equation [16], with the extracion of information of mammograms [17].

This paper presents a method of image classification based on application of Gabor filters followed by a neural network with back propagation algorithm, showing that the application of this method to satellite images results in classification with high accuracy. This method for classifying remote sensing images integrates the importance of textural attributes in selecting features with the efficiency of artificial neural networks in the classification process. A brief description of this method and some initial results were presented at a Brazilian congress [18].

2. Segmentation of textures with Gabor filters

Gabor [19] proved that the specification of a signal in the time domain and in the frequency domain is constrained by a lower bound, given by the equation (1), where Δt and $\Delta\omega$ can be understood as resolution respectively in the temporal and frequency domains.

$$\Delta t \cdot \Delta\omega \geq \frac{1}{4\pi} \tag{1}$$

Gabor also derived the family of functions that achieve this lower bound, as shown in the equation (2), that describes with a relatively simple expression a sine wave with frequency ω modulated by a Gaussian envelop of extent σ.

$$f(t) = \exp\left[-\frac{1}{2}\left(\frac{t}{\sigma}\right)^2 + i\omega t\right] \tag{2}$$

Daugman [20-22] extended the set of filters proposed by Gabor to two dimensional data, getting the equation (3), where u0 and v0 represent the selected spatial frequencies along respectively the x and y directions and σx and σy represent the spatial extents of the Gabor function also along the x and y directions.

$$f(x, y, u_0, v_0, \sigma_x, \sigma_y) = \frac{1}{2\pi\sigma_x\sigma_y}\exp\left\{-\frac{1}{2}\left[\left(\frac{x}{\sigma_x}\right)^2 + \left(\frac{y}{\sigma_y}\right)^2\right]\right\}\exp\{2\pi i[u_0 x + u_0 y]\} \tag{3}$$

The specification of a two dimensional signal simultaneously in the time and frequency domains is constrained as is shown in equation (4).

$$\Delta x \cdot \Delta y \cdot \Delta u \cdot \Delta v \geq \frac{1}{16\pi^2} \tag{4}$$

Equation (3) can be used to implement a set of filters to quantify the texture of the image to be classified. Angelo and Haertel [4] presented a supervised image classification method that uses the spatial texture attribute quantified by a set of Gabor filters. Indeed, the proposed procedure consists of a method for segmentation of textures, since the classification itself is implemented with a Gaussian maximum likelihood classifier. In this work, the classification is performed with a neural network.

3. Classification of images with a multi layer perceptron

The idea of neural networks had already been presented when Rosenblatt [23], in 1957, conceived the model of the perceptron, where the processing elements are divided into two layers completely interconnected. The intermediate layers began to be considered when Widrow and Hoff [24], in 1960, presented the adaline, the adaptive linear neuron.

The 70s saw the concept of neural networks fall into a relative oblivion until Hopfield [25] in 1982 proposed its use as a tool for optimization problems. From there, a new period of development began with the presentation of new concepts and new architectures for neural networks, approaching them from what can be understood as an artificial intelligence.

In 1986, Rumelhart and McClelland [26] added the idea of feedback to the training of multi-layer perceptrons. A network with intermediate layers for which, in the training phase, the outputs would be compared with the entries by determining an error. In later stages of training this error should be minimized.

The neural networks can be interpreted as changing data [27], where the point is the association of elements of one group of data with the elements of a second group of data. When applied to the classification, for instance, there is an interest in transforming data from the space of characteristics to the space of classes. As they belong to the same class of techniques as pattern recognition and linear regression, the neural networks have been frequently used in remote sensing, mainly because they allow handling large amounts of data.

The perceptron is one of the most widely used neural network in remote sensing. The multi layer perceptron can separate data that are non-linear and generally consists of three or more types of layers. In order to begin the learning process, it is necessary to select a set of samples of the classes of patterns, a training set, to be learned and the corresponding outputs obtained. Representative samples of each one of the classes must be chosen.

The number of neurons of the input and output layers is defined according to the problem that will be solved by the network. The number of hidden layers is defined intuitively and, therefore, no rule exists that will define their number. If a large number of neurons is defined, some neurons can become experts and others assume less importance. If the number of neurons is insufficient, the network may not have capacity to learn.

The major characteristic of this model is supervised learning based on two stages: propagation and adaptation. Training or supervised learning consists of supplying the network with a set of stimuli input patterns, and the corresponding desired output, where the first input pattern is propagated to the output.
In the adaptation phase, an error sign at the output is computed and transmitted back to each neuron of the hidden layer that contributed to that output. Thus, each neuron of the hidden layer receives only a part of the total error, according to the relative contribution that each neuron made to the output generated.
This process is repeated layer by layer until all neurons of the network have received their share of the error. This process is called backpropagation learning because it is based on backward propagation of the error for upper levels of the network as a feedback.
According to the error received by the associated neurons, the weights that exist in the connections between the neurons are updated. This learning rules is a generalization of the least mean square error rule, also known as delta rule.
With the due changes in weights, the learning process remains until the time when the output obtained by the neural network is close enough to the desired output, so that the difference between both is acceptable. This difference is obtained by calculating the mean square error. A difference is considered acceptable if it is less than or equal to a previously stipulated error (e.g., an average of 1% or 0.5%).

4. Experiments

The procedure proposed in this work was tested in six experiments. A synthetic image was used in the first four experiments and a true picture, obtained by remote sensing, was used in the other two. The first is shown in Figure 1 (a) and the second in Figure 11 (a), both with dimensions of 256 by 256 pixels. The synthetic image was obtained from real textures extracted from the photographic album of Brodatz [28], including four different textures. The real image, a digitized, raster-shaped image of the metropolitan area of the municipality of Porto Alegre (http://goo.gl/maps/uDsCh), in southern Brazil, is characterized by three different classes of texture.
The experiments were conducted on five well-defined phases. First, selection of samples of the main classes of image. In the case of real images, it is more effective to select samples of the most important classes, despite suggestions [4] to select samples of all classes. Second step, identification of the spatial frequencies u and v which allow a better discrimination between the classes associated with the selected samples. And further, an investigation of the spatial extents σx and σy of the Gabor filters in terms of accuracy of the segmentation process. Third, convolution of the image with the bank of Gabor filters, generating a number of "textural bands" equal to the number of selected filters. Fourth, training of the multi layer neural network with back propagation algorithm to constitute the classifier. And, finally, the image classification, with the use of "textural bands" to generate a thematic image.
Filtering through the Gabor filters, as well as the classification of the resulting filtered images by the neural network was processed using MATLAB for Windows [29] software, developed by Math Works, Inc., version 5.3. Even being an older version, it loses to the latest versions mostly in the user interface characteristics.
Each class in the images should lead to at least one sample. The choice of the sample should ensure selection of patterns representing the class from which it was obtained. In the synthetic image was obtained one sample per class (Figure 1(b)). In real image were obtained five samples per class (Figure 11 (b)).
The selection of frequencies to determine the Gabor filters in each experiment is performed based on the frequencies of each sample that present the highest levels of energy. This frequency selection process is carried out based on the Fourier spectrum of each sample of each class of the images.
The application of filters on the image will generate a number of new images equal to the number of filters. The number of filtered images defines the number of neurons in the input layer. The number of classes to be classified defines the number of neurons in the output layer. The number of neurons in intermediate layer may vary for each experiment.
The classification of the image by neural network will take place by means of a pixel to pixel process, where the neural network input parameters will be the values of each pixel of the "textural bands". The activation function selected for the neural network was the hyperbolic tangent function, since it converges faster. The backpropagation algorithm is based on the descending gradient from error, with minimization of the mean quadratic error.

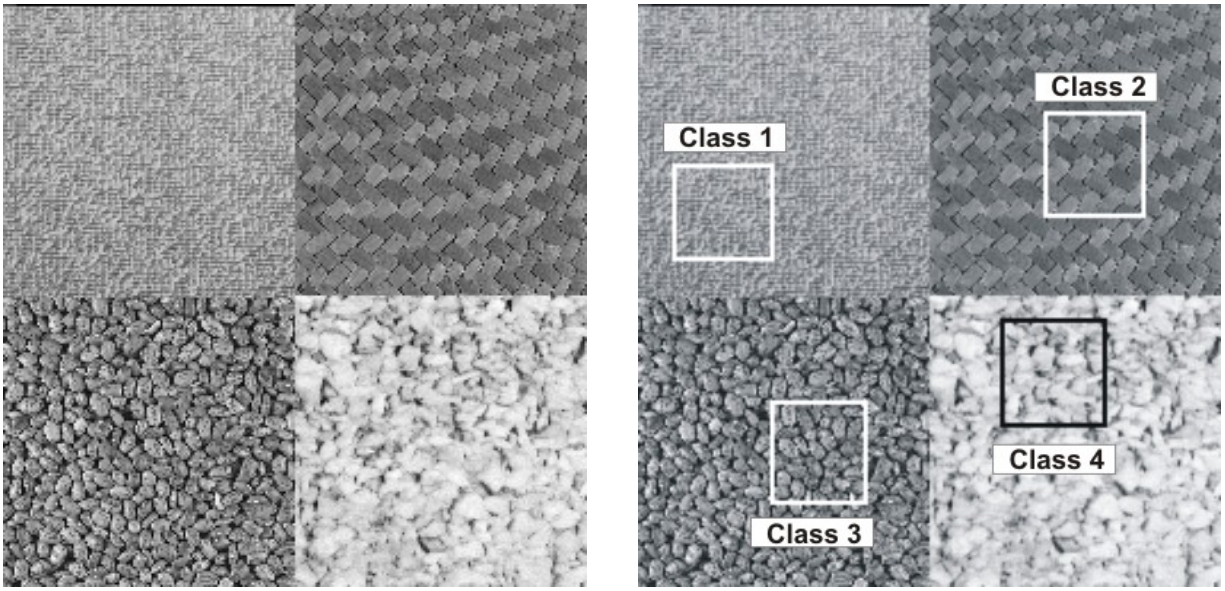

(a) (b)

Figure 1. (a) Synthetic image consisting of four classes defined by textures extracted from the Brodatz album, with 256 by 256 pixels; (b) Image with the location of the samples for the selection of features

The classification process is carried out directly based on the levels of gray of the pixels of each of the images resulting from processing by the Gabor filters. Therefore, each neuron of the input layer receives the information from the same pixel referring to each of the filtered images. The number of neurons of the network output layer will be equal to the number of classes existing in the image.

It were performed four experiments with Figure 1 (a), named A, B, C and D. Experiments A and B were performed with 15 filters, while experiments C and D with 25 filters. Experiments A and C were conducted with filters of different sizes, while experiments B and D were performed with filters of the same size.

For these experiments, neural networks have respectively 15 and 25 neurons in the input layer and 4 neurons in the output layer, since there are four different textures to be identified. Then, each of the four experiments was repeated twice, called respectively A1, A2; B1, B2; C1, C2 and D1, D2. Experiments A1 and A2 were performed respectively with 18 to 23 neurons in the hidden layer, experiments B1 and B2 with 18 and 23 and experiments C1, D1 and C2, D2 respectively with 28 and 32 neurons in the hidden layer.

It were performed two experiments with Figure 11 (a), named E and F. Experiment E were performed with 18 filters, while experiment F with 32 filters, both with filters of different sizes. Neural networks have respectively 18 and 32 neurons in the input layer and 3 neurons in the output layer, since there are three different textures to be identified. Then, each of the two experiments was repeated twice, called respectively E1, E2 and F1, F2. Experiments E1 and E2 were performed respectively with 20 to 25 neurons in the hidden layer and experiments F1 and F2 respectively with 35 and 40 neurons in the hidden layer.

5. Results and discussion

Considering the first four experiments, the samples of the Figure 1 (a) is shown in Figure 1 (b). Figure 2 shows the samples for each one of the four classes, their Fourier spectrum and frequencies that have the highest energy levels.

For the experiment A, the parameters needed for the constitution of Gabor filters appear in Table 1. The 15 Gabor filters of this table generated 15 filtered images, shown in Figure 3. The results of experiments A1 and A2 are shown respectively in Figure 4 (a) and Figure 4 (b). These images present respectively 88.65% and 82.94% of the pixels successfully identified. In these two figures, there was a reasonable identification of the limits of each texture and classified image textural characteristics were very similar to the original image (Figure 1 (a)). The first of these two figures may be singled out as the best classified image obtained with the first four experiments.

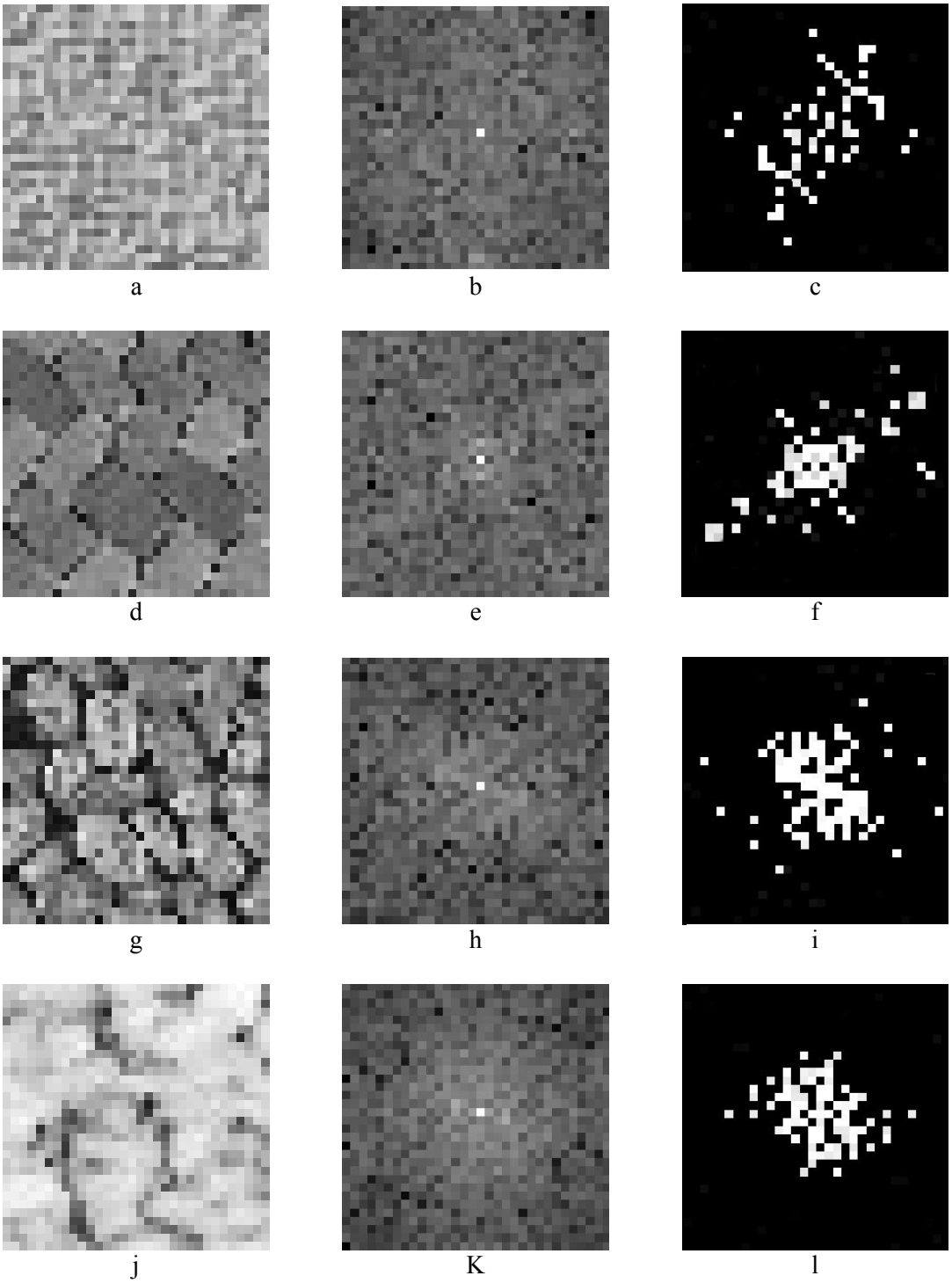

Figure 2. (a) Sample, (b) Fourier spectrum and (c) frequencies with highest energy levels of sample of class 1. (d) Sample, (e) Fourier spectrum and (f) frequencies with highest energy levels of sample of class 2. (g) Sample, (h) Fourier spectrum and (i) frequencies with highest energy levels of sample of class 3. (j) Sample, (k) Fourier spectrum and (l) frequencies with highest energy levels of sample of class 4

For the next experiment, the classification was implemented with filters constituted with the maximum value of spatial extent of the filters in Table 1. For the experiment B, the parameters needed for the filters appear in Table 2. The 15 Gabor filters of this table generated 15 filtered images, shown in Figure 5. The results of experiments B1 and B2 are shown in Figure 6 (a) and Figure 6 (b). These images present respectively 84.24% and 81.55% of the pixels successfully identified. In these two figures, there was some difficulty in identifying the limits of classes 1 and 3 and the classified images does not appear similar to the original image (Figure 1 (a)).

Table 1. Parameters for Gabor filters of the experiment A

Filter	Dimension (pixels)	Frequency along the x axis (k_x)	Frequency along the y axis (k_y)	Spatial extent (σ)
1	36	0,0532	0,0279	6,0000
2	34	0,0414	0,0296	5,6667
3	19	0,0549	0	3,1667
4	48	0,0211	0,0718	8,0000
5	29	0,0346	-0,1715	4,8333
6	44	0,0228	-0,0059	7,3333
7	44	0,0228	-0,1563	7,3333
8	18	0,0566	0,0718	3,0000
9	40	0,0253	-0,0282	6,6667
10	79	0,0127	0	13,1667
11	90	0	0,0602	15,0000
12	90	0,0112	0	15,0000
13	115	0,0087	0,0201	19,1667
14	115	0	0,0300	19,1667
15	115	0,0087	0,0391	19,1667

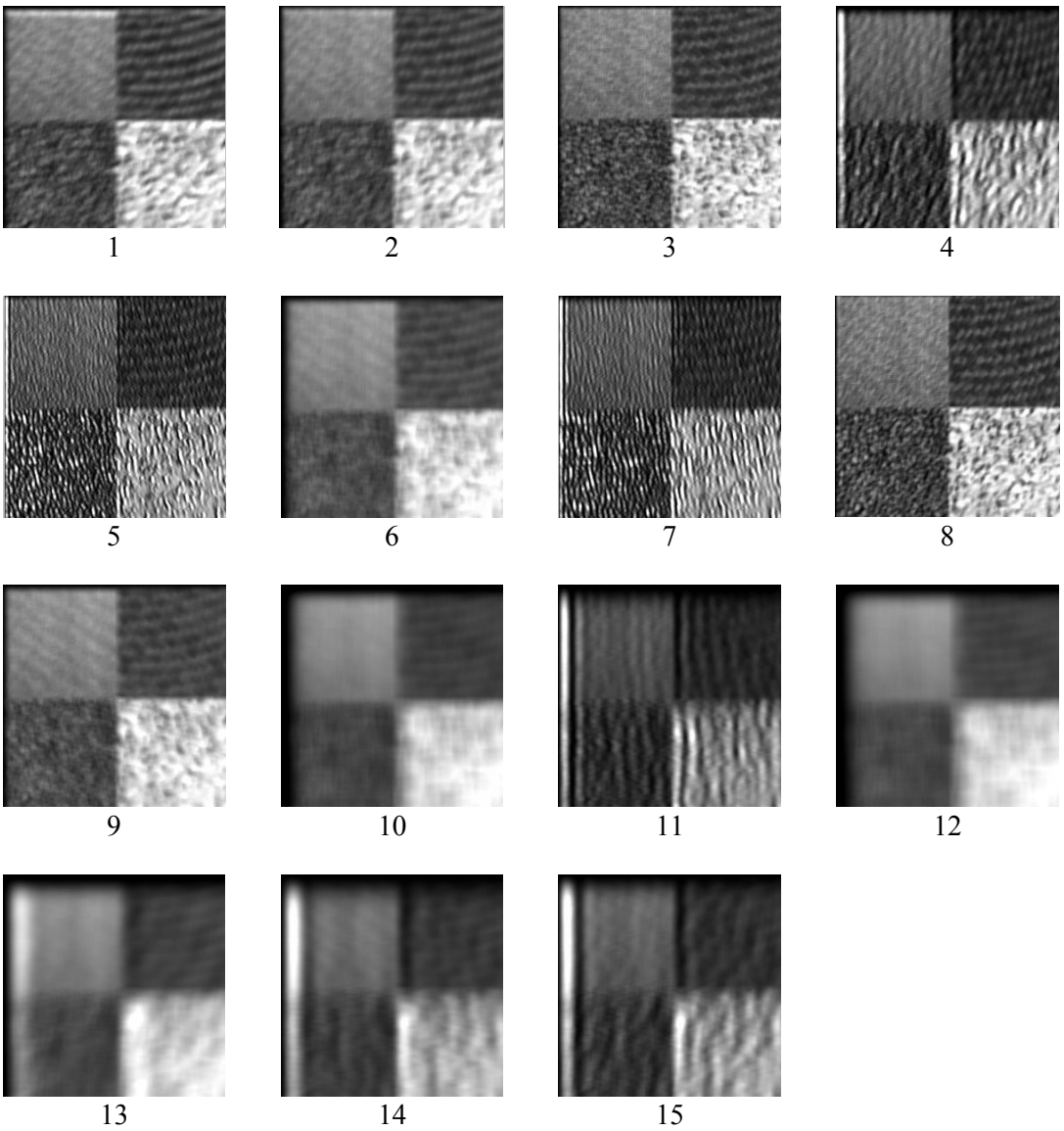

Figure 3. Filtered images obtained with the application of Gabor filters for the experiment A

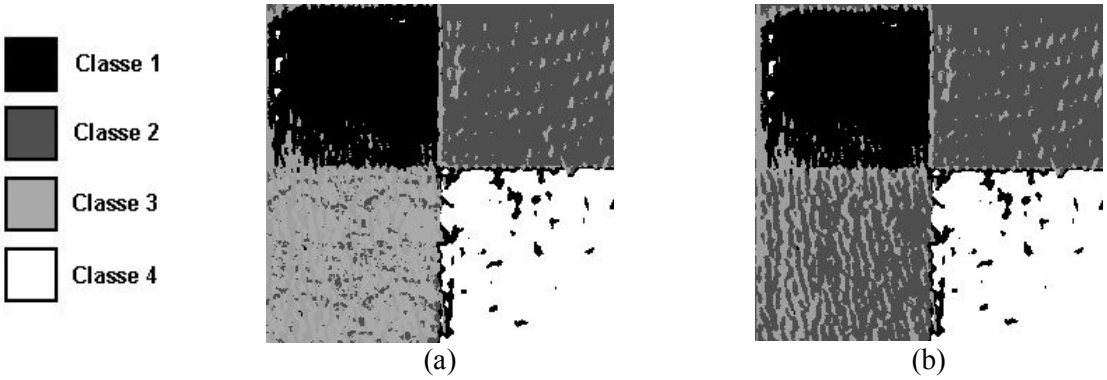

Figure 4. (a) Image classified on the experiment A1; (b) Image classified on the experiment A2

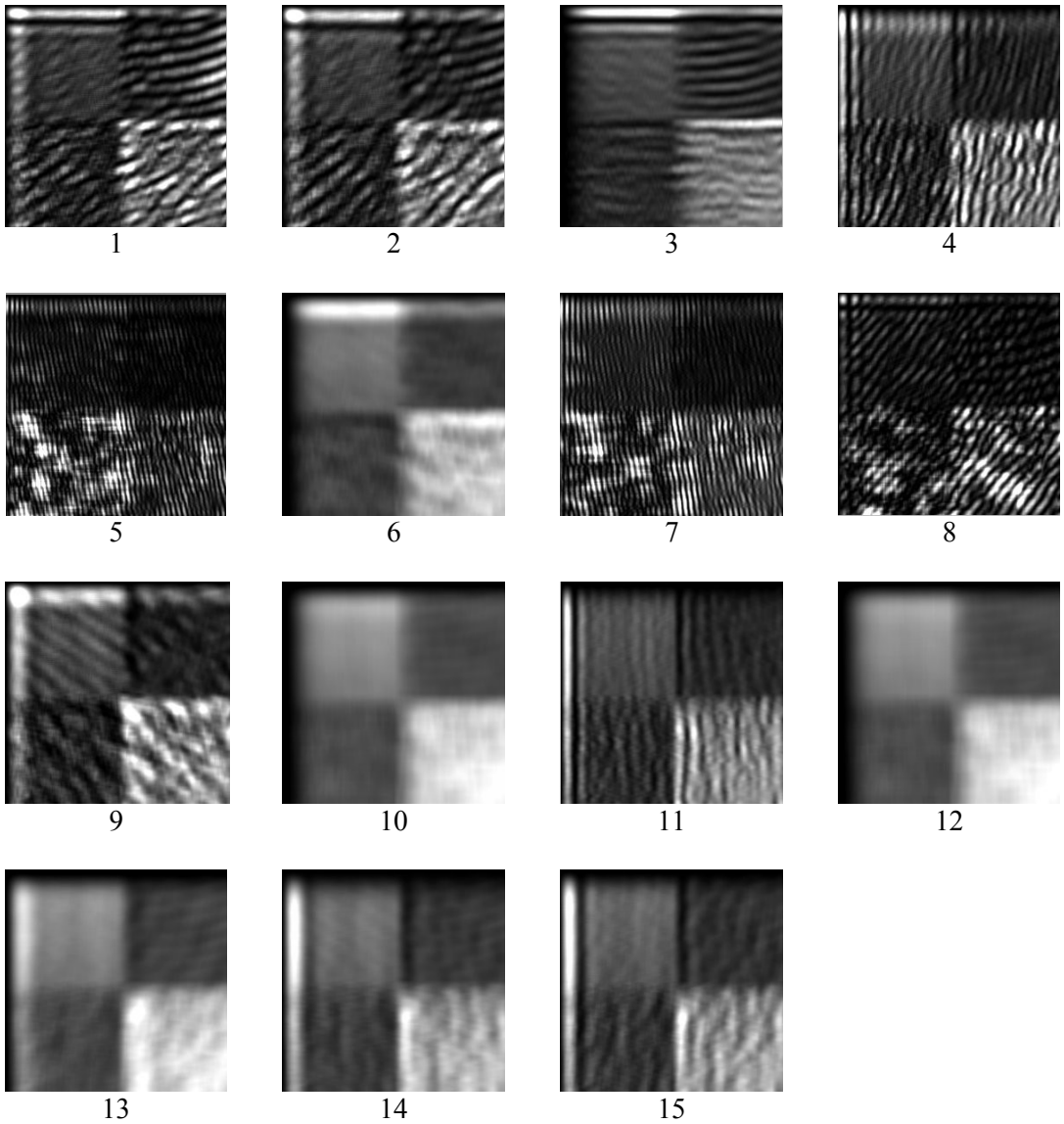

Figure 5. Filtered images obtained with the application of Gabor filters for the experiment B

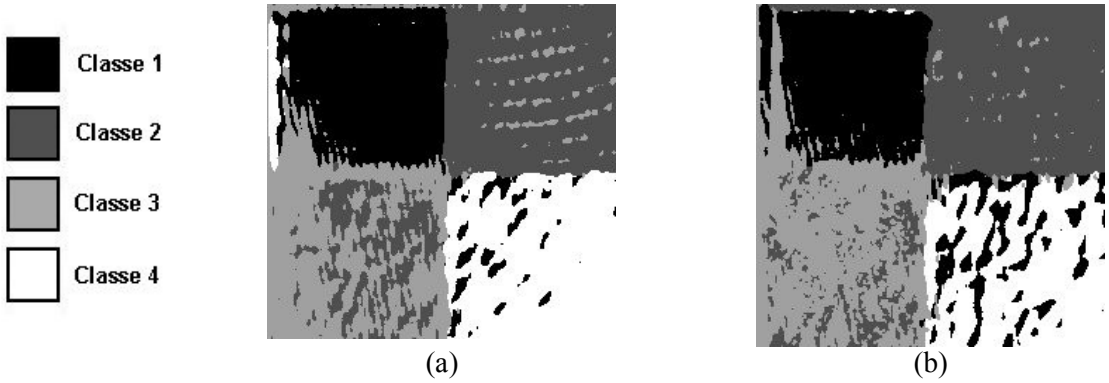

Figure 6. (a) Image classified on the experiment B1; (b) Image classified on the experiment B2

Table 2. Parameters for Gabor filters of the experiment B

Filter	Dimension (pixels)	Frequency along the x axis (k_x)	Frequency along the y axis (k_y)	Spatial extent (σ)
1	115	0,0532	0,0279	19,1667
2	115	0,0414	0,0296	19,1667
3	115	0,0549	0	19,1667
4	115	0,0211	0,0718	19,1667
5	115	0,0346	-0,1715	19,1667
6	115	0,0228	-0,0059	19,1667
7	115	0,0228	-0,1563	19,1667
8	115	0,0566	0,0718	19,1667
9	115	0,0253	-0,0282	19,1667
10	115	0,0127	0	19,1667
11	115	0	0,0602	19,1667
12	115	0,0112	0	19,1667
13	115	0,0087	0,0201	19,1667
14	115	0	0,0300	19,1667
15	115	0,0087	0,0391	19,1667

The next two experiments were carried out with 25 filters. For the experiment C, the parameters for the filters are shown in Table 3. The 25 Gabor filters of this table generated 25 filtered images, shown in Figure 7. The results of experiments C1 and C2 are shown in Figure 8 (a) and (b). These images present respectively 83.06% and 76.88% of the pixels successfully identified. In these figures, there was a good identification of the limits of the classes and the image keeping a good similarity with the original image (Figure 1 (a)), despite the relatively low number of pixels successfully identified in the second figure.
For the experiment D, the classification was implemented with filters constituted with the maximum value of spatial extent of the filters in Table 3. The parameters for the filters appear in Table 4. The 25 Gabor filters of this table generated 25 filtered images, shown in Figure 9. The results of experiments D1 and D2 are shown in Figure 10 (a) and (b). These images present 89.05%, the best result obtained in all experiments, and 87.37% of the pixels successfully identified. In the first of these two figures, there was an excellent identification of the limits of the classes and the image keeping an excellent similarity to the original figure, and also an optimum number of pixels successfully identified. The second image presented a problem in the left edge, although also present a good number of pixels identified.
Considering the last two of six experiments, the samples of the Figure 11 (a) are shown in Figure 11 (b) for class "water", Figure 11 (c) for "urban" and Figure 11 (d) for "vegetation". The urban area corresponds to the area of the city of Porto Alegre, the water class is the region of the Guaíba lake, and the vegetation concerns the area constituted by the islands in the estuary of the river Jacuí. Figure 12, Figure 13 and Figure 14 shows all the samples for each one of these three classes, their Fourier spectrum and frequencies that have the highest energy levels.

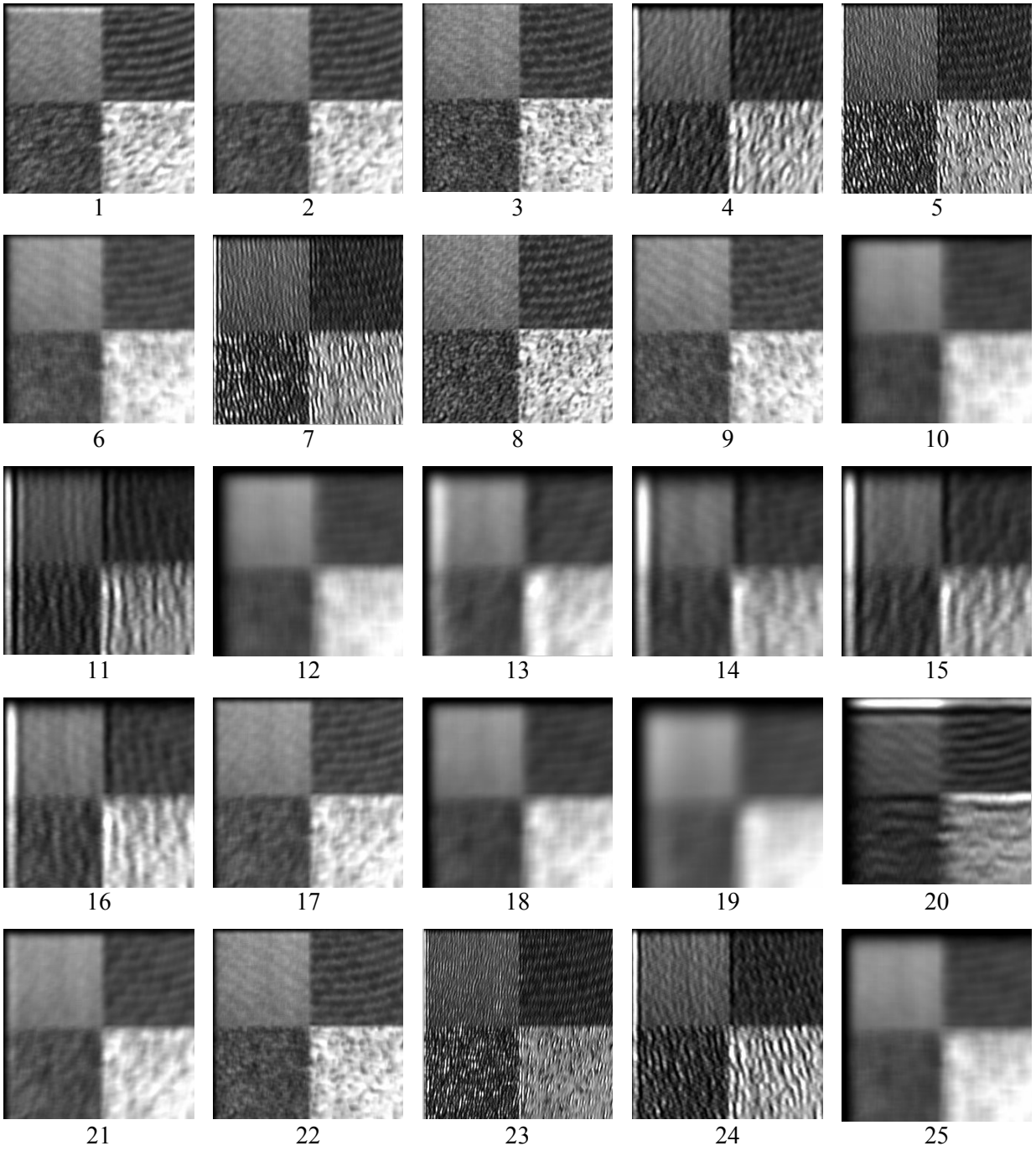

Figure 7. Filtered images obtained with the application of Gabor filters for the experiment C

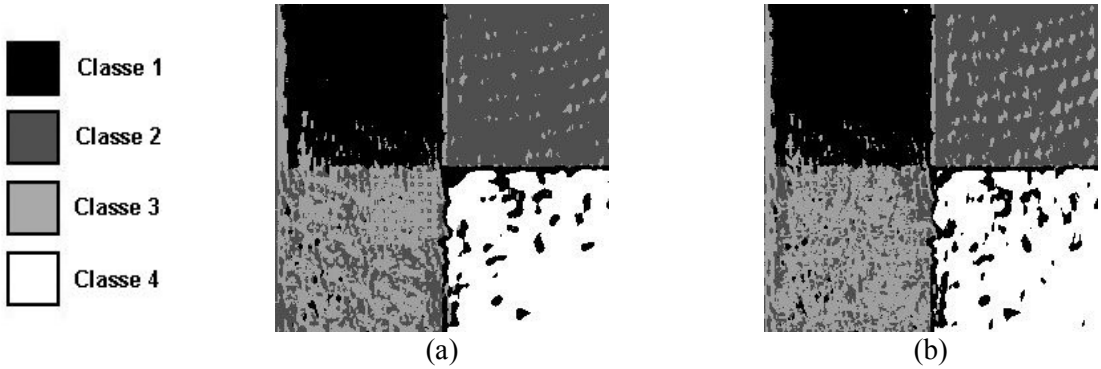

Figure 8. (a) Image classified on the experiment C1; (b) Image classified on the experiment C2

Table 3. Parameters for Gabor filters of the experiment C

Filter	Dimension (pixels)	Frequency along the x axis (k_x)	Frequency along the y axis (k_y)	Spatial extent (σ)
1	36	0,0532	0,0279	6,0000
2	34	0,0414	0,0296	5,6667
3	19	0,0549	0	3,1667
4	48	0,0211	0,0718	8,0000
5	29	0,0346	-0,1715	4,8333
6	44	0,0228	-0,0059	7,3333
7	44	0,0228	-0,1563	7,3333
8	18	0,0566	0,0718	3,0000
9	40	0,0253	-0,0282	36,6667
10	79	0,0127	0	13,1667
11	90	0	0,0602	15,0000
12	90	0,0112	0	15,0000
13	115	0,0087	0,0201	19,1667
14	115	0	0,0300	19,1667
15	115	0,0087	0,0391	19,1667
16	79	0	0,0423	13,1667
17	43	0,0235	0,0267	7,1667
18	85	0,0118	0,0133	14,1667
19	145	0,0069	0,0109	24,1667
20	102	0,0443	0	17,0000
21	57	0,0177	0,0291	9,5000
22	29	0,0353	-0,0133	4,8333
23	30	0,0338	0,2500	5,0000
24	50	0,0203	-0,0878	8,3333
25	85	0	0,0133	14,1667

Table 4. Parameters for Gabor filters of the experiment D

Filter	Dimension (pixels)	Frequency along the x axis (k_x)	Frequency along the y axis (k_y)	Spatial extent (σ)
1	220	0,0532	0,0279	36,6667
2	220	0,0414	0,0296	36,6667
3	220	0,0549	0	36,6667
4	220	0,0211	0,0718	36,6667
5	220	0,0346	-0,1715	36,6667
6	220	0,0228	-0,0059	36,6667
7	220	0,0228	-0,1563	36,6667
8	220	0,0566	0,0718	36,6667
9	220	0,0253	-0,0282	36,6667
10	220	0,0127	0	36,6667
11	220	0	0,0602	36,6667
12	220	0,0112	0	36,6667
13	220	0,0087	0,0201	36,6667
14	220	0	0,0300	36,6667
15	220	0,0087	0,0391	36,6667
16	220	0	0,0423	36,6667
17	220	0,0235	0,0267	36,6667
18	220	0,0118	0,0133	36,6667
19	220	0,0069	0,0109	36,6667
20	220	0,0443	0	36,6667
21	220	0,0177	0,0291	36,6667
22	220	0,0353	-0,0133	36,6667
23	220	0,0338	0,2500	36,6667
24	220	0,0203	-0,0878	36,6667
25	220	0	0,0133	36,6667

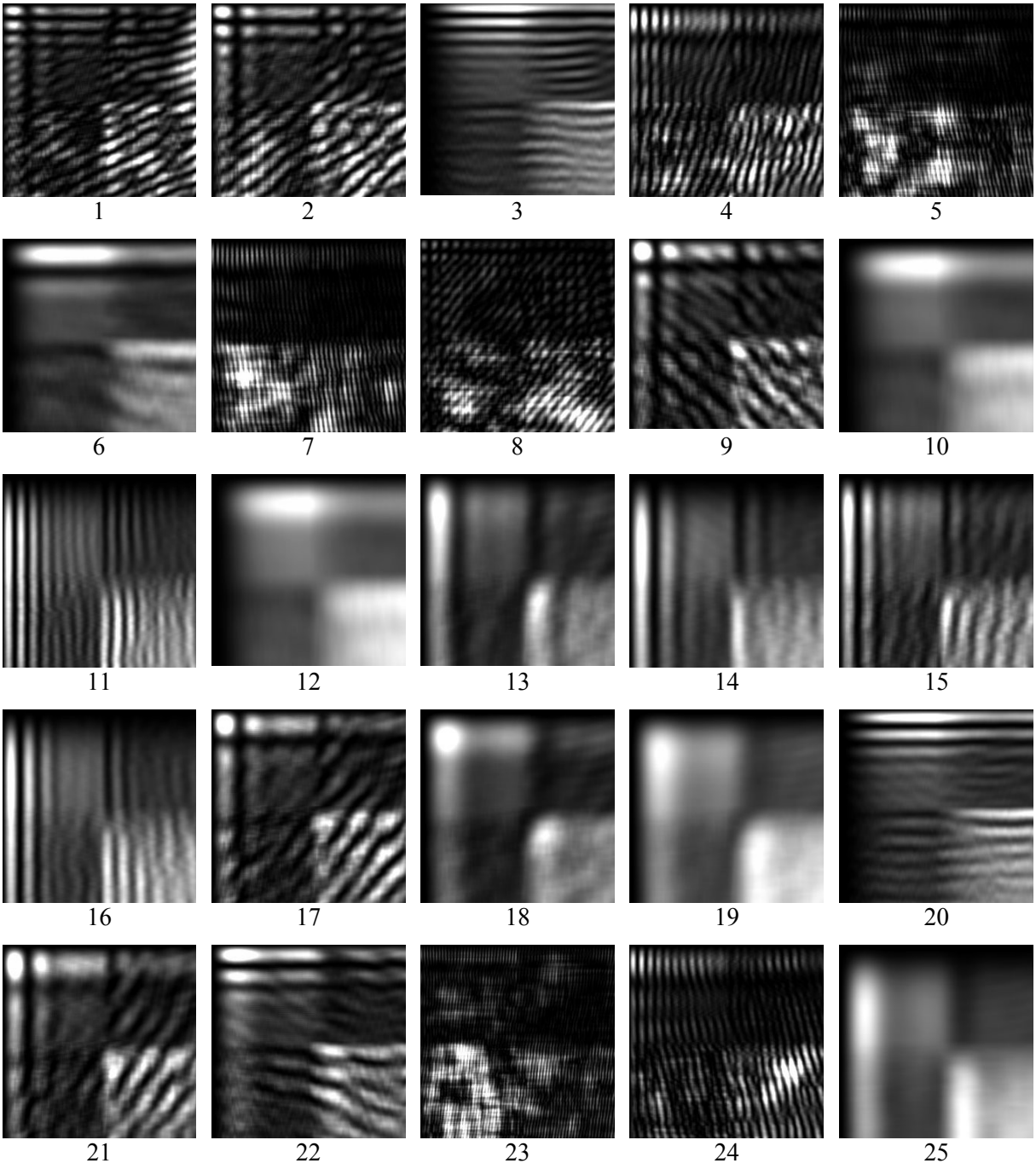

Figure 9. Filtered images obtained with the application of Gabor filters for the experiment D

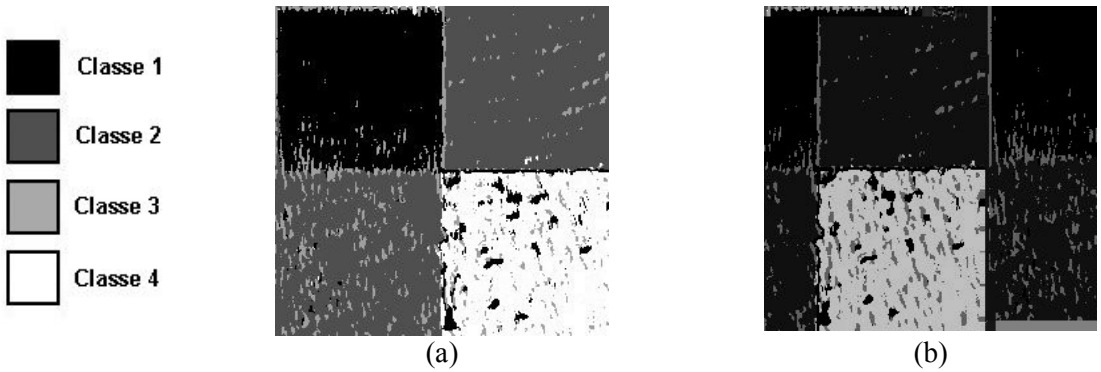

Figure 10. (a) Image classified on the experiment D1; (b) Image classified on the experiment D2

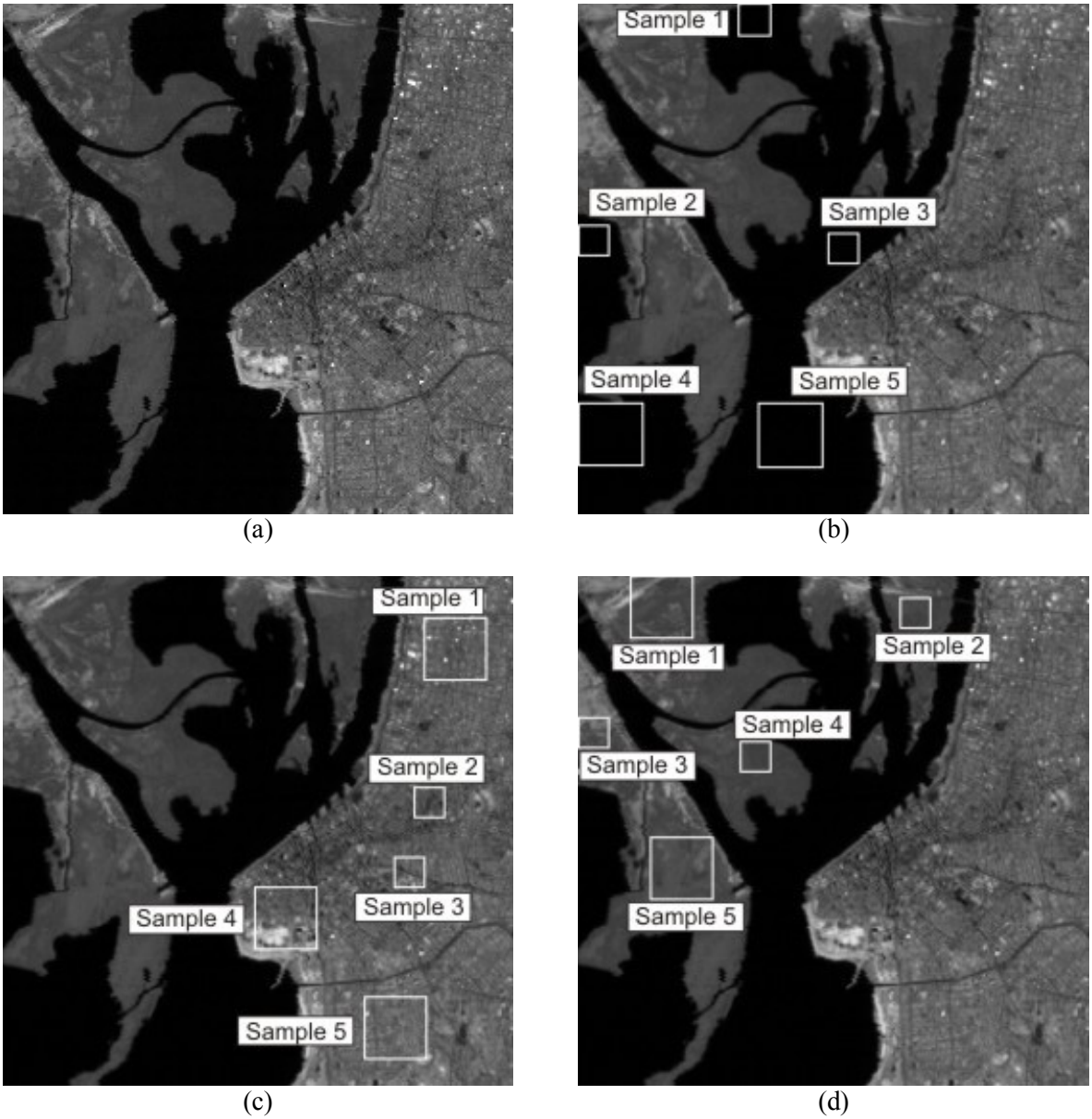

Figure 11. (a) Digital image of the city of Porto Alegre; (b) Image with location of representative samples of class "water" for selection of textures; (c) Image with location of representative samples of class "urban" for selection of textures; (d) Image with location of representative samples of class "vegetation" for selection of textures.

For the experiment E, the parameters for the filters appear in Table 5. The 18 Gabor filters of this table generated 18 filtered images, shown in Figure 15. The results of experiments E1 and E2 are shown in Figure 16 (a) and (b). The first of these figures presented 85.15% of the pixels successfully identified, the best result of the experiments of this step. The other presented 83.38% of the pixels successfully identified. In these two classified images, it was obtained a good similarity to the original image, including an excellent identification of boundaries between the classes. In this kind of image, a good identification of boundaries represents a proper identification of characteristics of the terrain. It was observed a good capacity for the differentiation of the class water, but difficulty in the differentiation of the other two classes, urban and vegetation.

For the experiment F, the parameters for the filters appear in Table 6. The 32 Gabor filters of this table generated 32 filtered images, shown in Figure 17. This experiment evaluates the effect introduced by the increase in the number of Gabor filters. As can be seen below, the increase in the number of filters not led to an increase of accuracy. The results of experiments F1 and F2 are shown in Figure 18 (a) and (b).

These images present respectively 82.57% and 82.49% of the pixels successfully identified. As in the previous classified images, it was observed some difficulty in the differentiation of classes urban and vegetation, but a good accuracy in the identification of the features of class water.

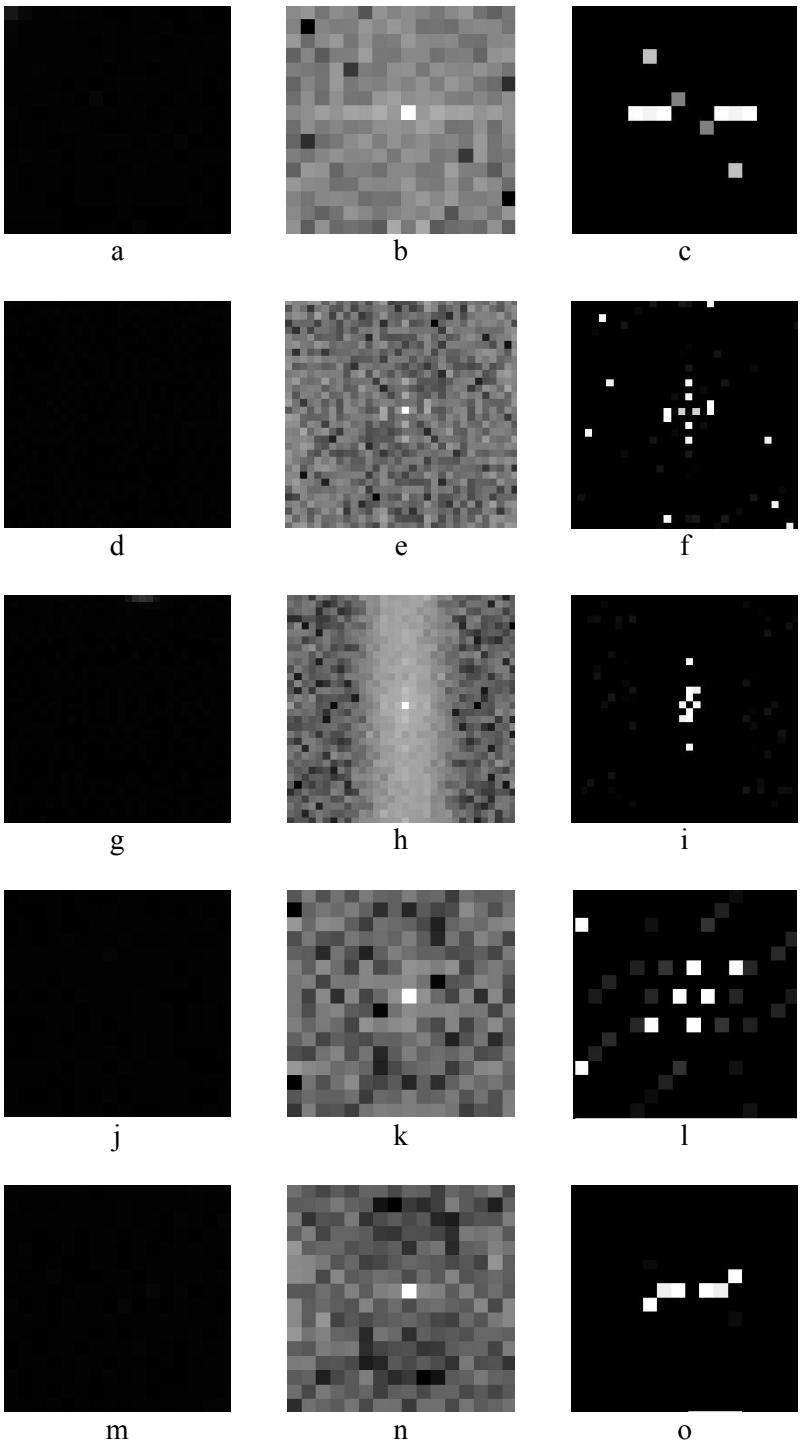

Figure 12. (a) Sample, (b) Fourier spectrum and (c) frequencies with highest energy levels of sample 1 of class water (Figure 15 (b)). (d) Sample, (e) Fourier spectrum and (f) frequencies with highest energy levels of sample 2 of class water (Figure 15 (b)). (g) Sample, (h) Fourier spectrum and (i) frequencies with highest energy levels of sample 3 of class water (Figure 15 (b)). (j) Sample, (k) Fourier spectrum and (l) frequencies with highest energy levels of sample 4 of class water (Figure 15 (b)). (m) Sample, (n) Fourier spectrum and (o) frequencies with highest energy levels of sample 5 of class water (Figure 15 (b))

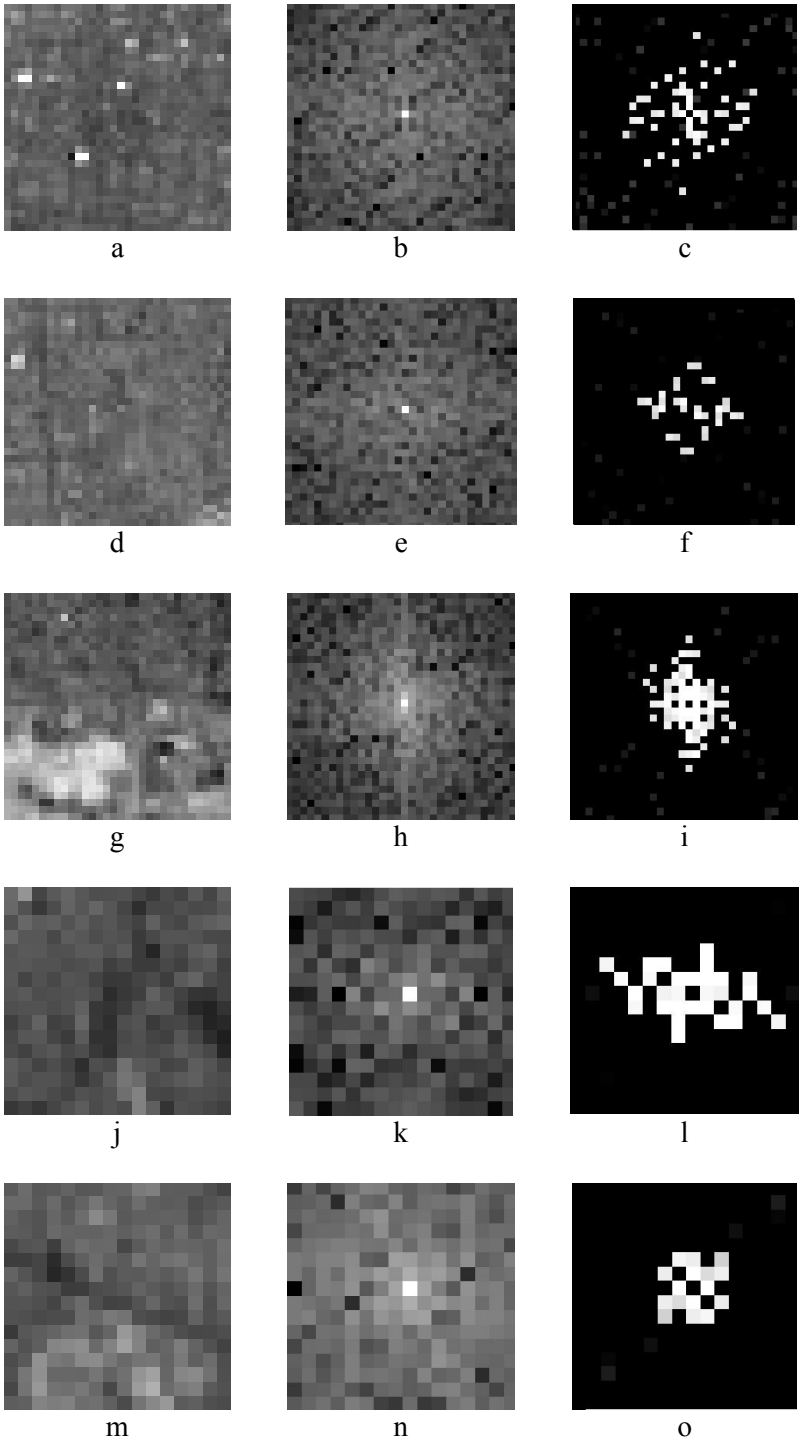

Figure 13. (a) Sample, (b) Fourier spectrum and (c) frequencies with highest energy levels of sample 1 of class urban (Figure 15 (c)). (d) Sample, (e) Fourier spectrum and (f) frequencies with highest energy levels of sample 2 of class urban (Figure 15 (c)). (g) Sample, (h) Fourier spectrum and (i) frequencies with highest energy levels of sample 3 of class urban (Figure 15 (c)). (j) Sample, (k) Fourier spectrum and (l) frequencies with highest energy levels of sample 4 of class urban (Figure 15 (c)). (m) Sample, (n) Fourier spectrum and (o) frequencies with highest energy levels of sample 5 of class urban (Figure 15 (c)).

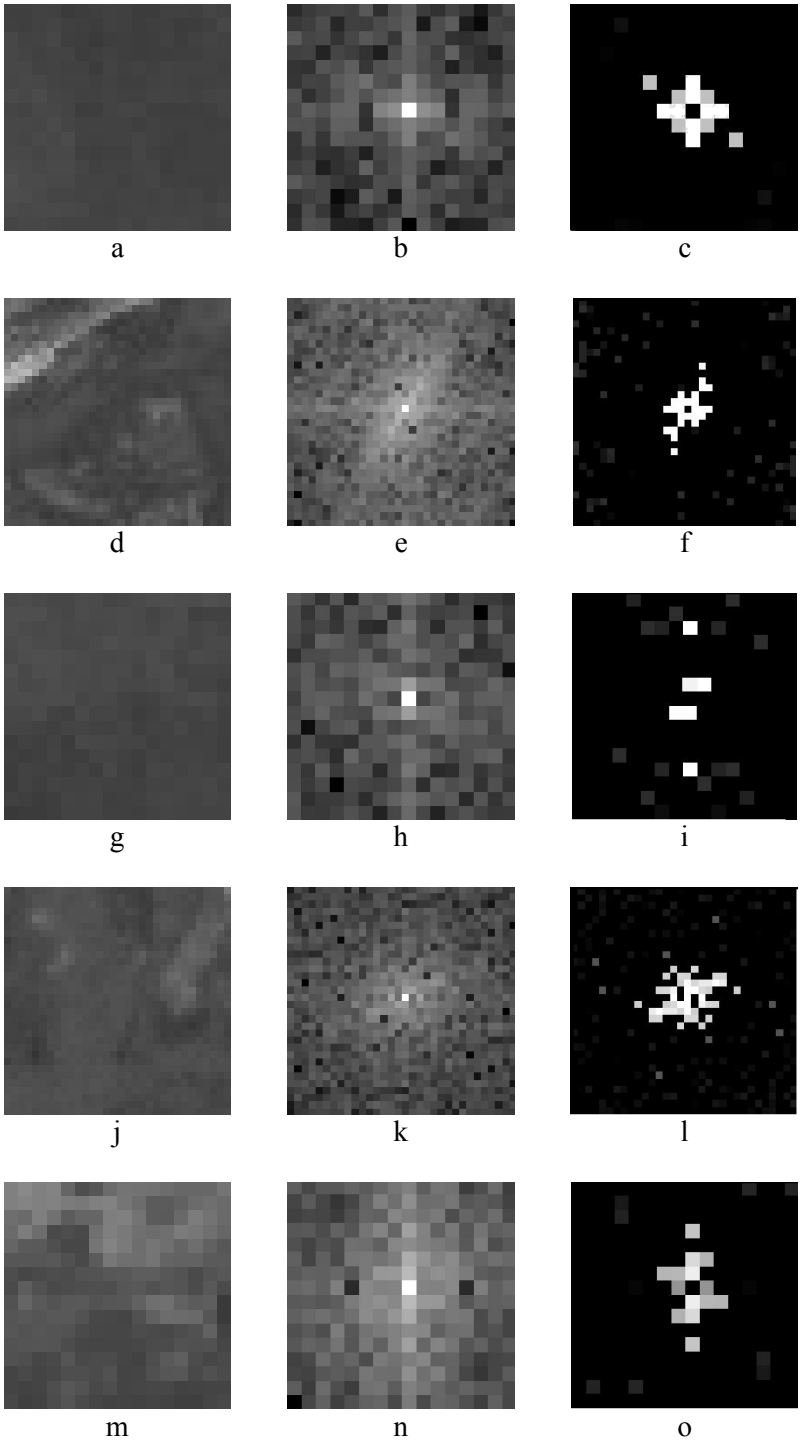

Figure 14. (a) Sample, (b) Fourier spectrum and (c) frequencies with highest energy levels of sample 1 of class vegetation (Figure 15 (d)). (d) Sample, (e) Fourier spectrum and (f) frequencies with highest energy levels of sample 2 of class vegetation (Figure 15 (d)). (g) Sample, (h) Fourier spectrum and (i) frequencies with highest energy levels of sample 3 of class vegetation (Figure 15 (d)). (j) Sample, (k) Fourier spectrum and (l) frequencies with highest energy levels of sample 4 of class vegetation (Figure 15 (d)). (m) Sample, (n) Fourier spectrum and (o) frequencies with highest energy levels of sample 5 of class vegetation (Figure 15 (d))

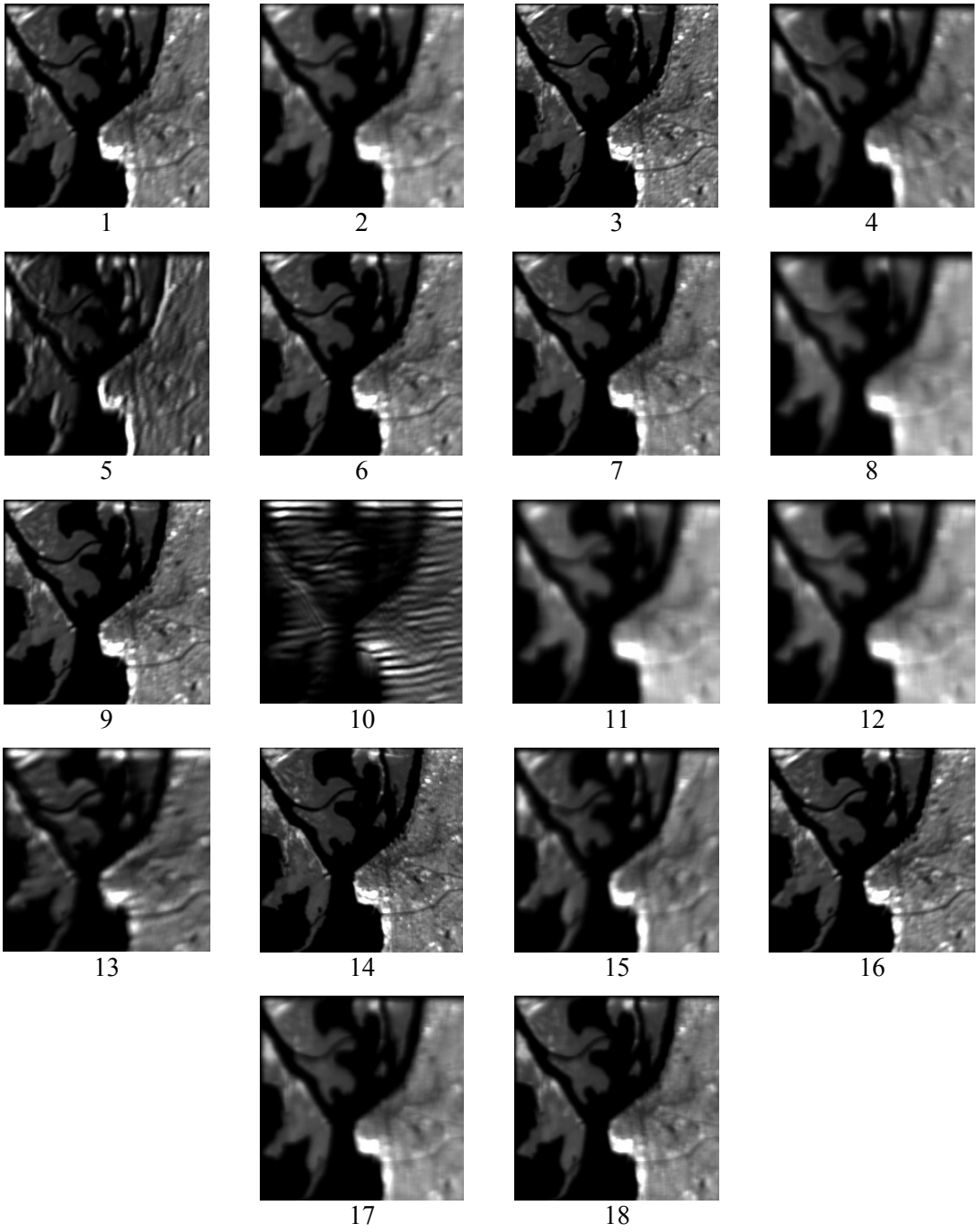

Figure 15. Filtered images obtained with the application of Gabor filters for the experiment E

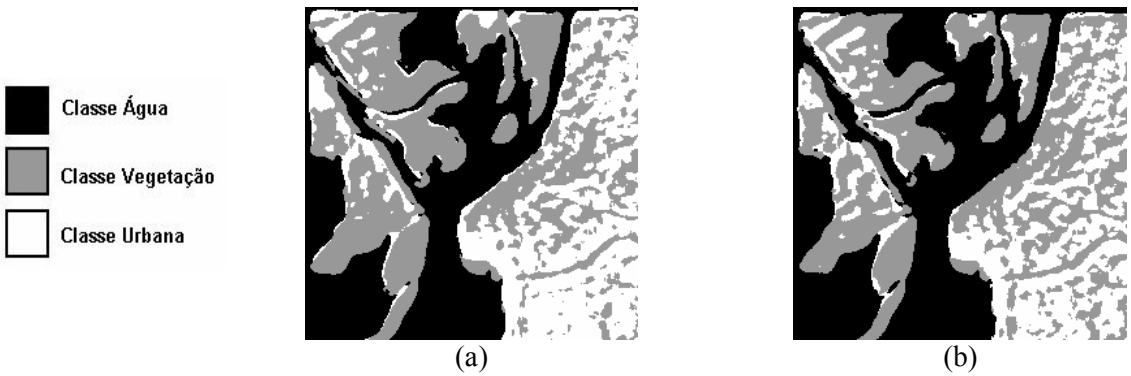

Figure 16. (a) Image classified on the experiment E1; (b) Image classified on the experiment E2

Table 5. Parameters for Gabor filters of the experiment E, with a real image

Filter	Dimension (pixels)	Frequency along the x axis (k_x)	Frequency along the y axis (k_y)	Spatial extent (σ)
1	27	0,0380	0,0600	4,5000
2	36	0,0285	0,0280	6,0000
3	17	0,0853	0,0617	2,8333
4	52	0,0194	-0,0296	8,6667
5	47	0,0215	0,0731	7,8333
6	27	0,0503	0,0376	4,5000
7	25	0	0,0405	4,1667
8	64	0	0,0157	10,6667
9	21	0,0621	0,0477	3,5000
10	108	0,0830	0,0093	18,0000
11	96	0,0105	0	16,0000
12	58	0,0173	0	9,6667
13	53	0,0477	0,0190	8,8333
14	15	0,0678	-0,0333	2,5000
15	49	0,0207	0,0384	8,1667
16	25	0,0655	0,0401	4,1667
17	39	0	0,0258	6,5000
18	29	0	0,0346	4,8333

Table 6. Parameters for Gabor filters of the experiment F, with a real image

Filter	Dimension (pixels)	Frequency along the x axis(k_x)	Frequency along the y axis (k_y)	Spatial extent (σ)
1	27	0,0380	0,0600	4,5000
2	36	0,0285	0,0280	6,0000
3	17	0,0853	0,0617	2,8333
4	52	0,0194	-0,0296	8,6667
5	47	0,0215	0,0731	7,8333
6	27	0,0503	0,0376	4,5000
7	25	0	0,0405	4,1667
8	64	0	0,0157	10,6667
9	21	0,0621	0,0477	3,5000
10	108	0,0830	0,0093	18,0000
11	96	0,0105	0	16,0000
12	58	0,0173	0	9,6667
13	53	0,0477	0,0190	8,8333
14	15	0,0678	-0,0333	2,5000
15	49	0,0207	0,0384	8,1667
16	25	0,0655	0,0401	4,1667
17	39	0	0,0258	6,5000
18	29	0	0,0346	4,8333
19	94	0,0107	0	15,6667
20	94	0,0107	-0,0150	15,6667
21	22	0,0455	-0,0364	3,6667
22	17	0,0588	0	2,8333
23	15	0,0678	-0,0333	2,5000
24	44	0,0232	-0,0055	7,3333
25	34	0,0298	0	5,6667
26	26	0,0393	0,0410	4,3333
27	8	0,1250	-0,1053	1,3333
28	56	0,0317	0,0179	9,3333
29	39	0,0256	0	6,5000
30	40	0	0,0579	6,6667
31	40	0	0,0789	6,6667
32	50	0	0,0400	8,3333

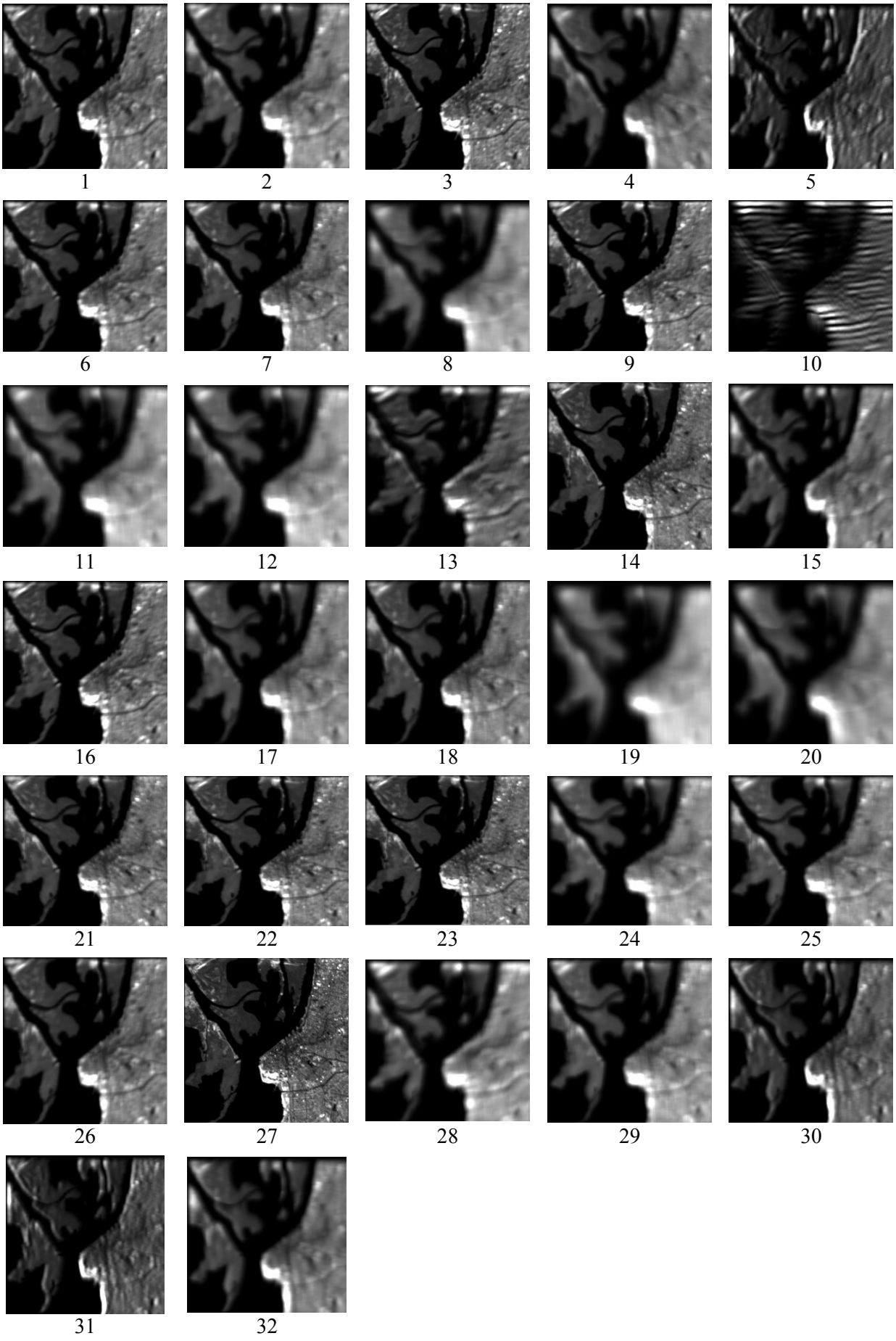

Figure 17. Filtered images obtained with the application of Gabor filters for the experiment F

Figure 18. (a) Image classified on the experiment F1; (b) Image classified on the experiment F2

Table 7 shows a comparison of the results of the six experiments. The results show a good accuracy, with values in the majority above 80%. The best result for the synthetic image was 89.05% and the real image was 85.15%. The trend is that fewer filters and fewer neurons in the hidden layer generate better results, with one exception.

Table 7. Comparative results of the six experiments. Specific spatial extension means extension selected in the process of formation of Gabor filters. Selected spatial extension means the maximum value achieved in the process of formation of Gabor filters

		Experiment	Number of filters	Spatial extension	Number of neurons per neural network layer			Accuracy
					Input	Hidden	Output	
Image	Synthetic	A1	15	Specific	15	18	4	88,65%
		A2	15		15	23	4	82,94%
		B1	15	Selected	15	18	4	84,24%
		B2	15		15	23	4	81,55%
		C1	25	Specific	25	28	4	83,06%
		C2	25		25	32	4	76,88%
		D1	25	Selected	25	28	4	89,05%
		D2	25		25	32	4	87,37%
	Real	E1	18	Specific	18	20	3	85,15%
		E2	18		18	25	3	83,38%
		F1	32	Specific	32	35	3	82,57%
		F2	32		32	40	3	82,49%

Clearly the influence of the number of filters on the results of the final classification. A larger number of filters for segmentation of textures, and hence of neurons in the initial layer of the neural network, leads to a lower accuracy of the final result.

Clearly also the influence of the number of neurons in the intermediate layer on the results of the final classification. A greater number of neurons in intermediate layer reduces the accuracy in the classification process. This worse accuracy may be caused by the existence of neurons surpluses to the network.

The exception was the experiment D, particularly D1, in which a larger number of filters and a smaller number of neurons in the hidden layer resulted in the best outcome for all experiments.

Another aspect that has shown to have an effect on the accuracy of the final result is the influence of the extension of the filters. The results show that the extension of the filters influences the classification accuracy in some experiments contributing to increased accuracy and other reducing the accuracy of the final result.

These results suggest the continuation of this study, to determine the influence of the number of filters and its extensions and the number of neurons in the hidden layer on the accuracy that can be achieved in the final result.

Throughout the study, it was observed that the choice of samples to obtain the spatial frequencies for each class is important for the success of the classification process. The more representative it is the selected sample of each class, best will be the selection of features. However, the large number of spatial frequencies and the possibility of the same frequency appear in different classes with distinct amplitudes may result in error in the classification process. This aspect needs to be better known.
Throughout the study, it was also observed that some frequencies not used in the preparation of filters influence the results obtained with a smaller number of filters. It was observed that the use of a single value for the spatial extent of the Gabor filters reduced the accuracy of the classification process. It is then suggested that a classification with a greater number of filters allied to appropriate spatial extent, could reduce the loss of information.
Then, the study should also be continued to explore the influence of the number of classes and the choice of samples on the accuracy of the process. And finally, perhaps most interestingly, also to study the influence of the frequencies and sub frequencies of the filters adopted on the accuracy of the process.

6. Conclusions

The purpose of this work was to present a method for classification of satellite images by texture using Gabor filtering for segmentation of textures and a multilayer neural network with a back propagation algorithm for the image classification. This method was applied to a synthetic image and an image obtained by remote sensing. Four experiments were carried out with the synthetic image and other two with the real image. The experiments were developed by well-defined phases: choice of samples in classes present in the image; extractions of characteristic frequencies for each textural class; formation of Gabor filters corresponding to each spatial frequency chosen; convolution of the image with each Gabor filter; training of the neural network to constitute the classifier based on a neural network; and, finally, image classification. The classification accuracy was measured by counting the number of pixels in the image that has been properly classified.
The results show a good accuracy, with values in the majority above 80%. The best result for the synthetic image was 89.05% and the real image was 85.15%. The trend is that fewer filters and fewer neurons in the hidden layer generate better results, with one exception. The extent and frequency of the filters also influence, of course, the classification accuracy. The choice of samples to obtain the spatial frequencies for each class is important for the success of the classification process, establishing the effectiveness of the classification method.
As a suggestion to continue the research, the method can achieve better accuracy in image classification from a better understanding of the influence of the number of filters and the number of neurons in the hidden layer on the classification result. The focus of the work should also be directed on frequencies and extensions of the filters adopted, as well as on techniques for choosing samples. Finally, it must be better understood the relationship between the extension of the filters and their frequencies and sub frequency.

References

[1] SKLANSKY, J., 1978, Image segmentation and feature extraction. IEEE Transactions on Systems, Man and Cybernetics, 13, 907-916.
[2] JAIN, A. K. and FARROKHNIA, F., 1991, Unsupervised texture segmentation using Gabor filters. Pattern Recognition, 24, 1167-1186.
[3] RAGHU, P. P., POONGODI, R. and YEGNANARAYANA, B., 1995, A combined neural network approach for texture classification. Neural Networks, 8, 975-987.
[4] ANGELO, N.P. and HAERTEL, V., 2003, On the application of Gabor filtering in supervised image classification. International Journal on Remote Sensing, 24, 2167-2189.
[5] DUNN, D. and HIGGINS, W. E., 1995, Optimal Gabor filters for texture segmentation. IEEE Transactions on Image Processing, 4, 947-964.
[6] WELDON, T. P., HIGGINS, W. E. and DUNN, D. F., 1996, Efficient Gabor filter design for texture segmentation. Pattern Recognition, 29, 2005-2015.
[7] RAGHU, P. P. and YEGNANARAYANA, B., 1996, Segmentation of Gabor-filtered textures using deterministic relaxation. IEEE Transactions on Image Processing, 5, 1625-1636.
[8] RAGHU, P. P. and YEGNANARAYANA, B., 1997, Multispectral image classification using Gabor filters and stochastic relaxation neural network. Neural Networks, 10, 561-572.

[9] RAGHU, P. P., POONGODI, R. and YEGNANARAYANA, B., 1997, Unsupervised texture classification using vector quantization and deterministic relaxation neural network. IEEE Transactions on Image Processing, 6, 1376-1387.
[10] RAGHU, P. P. and YEGNANARAYANA, B., 1998, Supervised texture classification using a probabilistic neural network and constraint satisfaction model. IEEE Transactions on Neural Networks, 10, 561-572.
[11] CALEANU, C., HUANG, D. S., GUI, V., TIPONUT, V. and MARANESCU, V., 2007, Interest Operator versus Gabor filtering for facial imagery classification. Pattern Recognition Letters, 28, 950-956.
[12] ANDRYSIAK, T., CHORAS, M., 2006, Image filtration and feature extraction for face recognition. Biometrics, Computer Security Systems and Artificial Intelligence Applications, p.3-12.
[13] MAYR, C., HEITTMANN, A. and SCHÜFFNY, R., 2007, Gabor-like image filtering using a neural microcircuit. IEEE Transactions on Neural networks, 18, 955-959.
[14] CANER, H., GECIM, S. and ALKAR, A.Z., 2008, Efficient embedded neural network based license plate recognition system. IEEE Transactions on Vehicular Technology, 57, 2675-2683.
[15] ZHU, B., JIANG, L., LUO, Y. and TAO, Y., 2007, Gabor feature-based apple quality inspection using kernel principal component analysis. Journal of Food Engineering, 81, 741-749.
[16] ADEDIJI, A., TUKUR, A.M., ADEPOJU, K.A., 2010, Assessment of Revised Universal Soil Loss Equation (RUSLE) in Katsina Area, Katsina State of Nigeria, using remote sensing and Geographic Information System. Iranica Journal of Energy and Environment, 1 (3): 255-264.
[17] WEI, C.H., LI, Y. LI, C.T., 2007, Effective extraction of Gabor features for adaptive mammogram retrieval. IEEE International Conference on Multimedia and Expo, p. 1503-1506.
[18] BELUCO, A., BELUCO, A., ENGEL, P.M., 2003, Classificação de imagens de sensoriamento remoto baseada em textura por redes neurais. Anais do XI Simpósio Brasileiro de Sensoriamento Remoto, Belo Horizonte, Brasil, p.1999-2006.
[19] GABOR, D., 1946, Theory of Communication. Journal of the Institute of Electrical Engineers, 93, 429-457.
[20] DAUGMAN, J. D., 1980, Two dimensional analysis of cortical receptive field profiles. Vision research, 20, 846-856.
[21] DAUGMAN, J. D., 1985, Uncertainty relation for resolution in space, spatial-frequency and orientation optimized by two dimensional visual cortical filters. Journal of the Optical Society of America-A, 2 (7), 1160-1169.
[22] DAUGMAN, J. D., 1988, Complete discrete 2-D Gabor transforms by neural networks for image analysis and compression. IEEE Transactions on Acoustics, Speech and Signal Processing, 36, 1169-1179.
[23] ROSENBLATT, F., 1958, The perceptron: A probabilistic model for information storage and organization in the brain. Psychological Review, 65 (3): 386-408.
[24] WIDROW, B., HOFF, M.E., 1960, Adaptive switching circuits. 1960 WESCON Convention Record, IV, p.96-104.
[25] HOPFIELD, J.J., 1982, Neural networks and physical systems with emergent collective computational abilities. Proceedings of the National Academy of Sciences of the united States of America, 79 (8): 2554-2558.
[26] RUMELHART, D.E, McCLELLAND, J.R., 1986, Parallel distributed processing. MIT Press: Cambridge, Massachussets, USA.
[27] PAO, Y. H., 1989, Adaptive pattern recognition and neural networks.Addison-Wesley: New York, USA, 301p.
[28] BRODATZ, P. T., 1966, Textures: a photogrametric album for artists and designers. New York: Dover, 143p.
[29] Mathworks, MATLAB, version 5.3, 1999.

Adriano Beluco has a Degree in Mathematics and a M.Sc. in Business Administration from Universidade Federal do Rio Grande do Sul, Porto Alegre, Brazil. He was a business consultant for over ten years, providing services in the areas of financial management and business valuation . He was financial mathematics teacher in educational institutions between 1998 and 2013. Since 2013 teaches at the Federal Institute of Rio Grande do Sul.
E-mail address: adbeluco@gmail.com

Paulo M. Engel is Electrical Engineer from the Federal University of Rio Grande do Sul (1978), MSc. on Microelectronics from the Polytechnic School of the University of São Paulo (1981) and Dr. Ing. on Microelectronics from Technical University Munich, Germany (1986). He has Posdocs in the field of Artificial Neural Networks: at the INP Grenoble, France (1990); at the TH Darmstadt, Germany (1991,1992). Since 1985 an active professor for Computer Science at the Federal University of Rio Grande do Sul.
E-mail address: engel@inf.ufrgs.br

Alexandre Beluco is Doctor of Engineering, Civil Engineering and BS in Physics, and is a professor at the Institute of Hydraulic Research (IPH), UFRGS, and has activity as a researcher on renewable energy resources. He teaches courses on hydraulics and on design methods for undergraduate engineering and on planning and evaluation of experiments and on methods of design and research for the graduate course in water resources, for which also offers elective courses on natural resources and renewable energy. Currently, he serves as reviewer of Energy, Solar Energy and Renewable and Sustainable Energy Reviews and had an article recently cited by Renewable Energy Global Innovations.
E-mail address: albeluco@iph.ufrgs.br